

UC San Diego

UC San Diego Previously Published Works

Title

Acoustic vector sensor beamforming reduces masking from underwater industrial noise during passive monitoring

Permalink

<https://escholarship.org/uc/item/88w0j07n>

Journal

The Journal of the Acoustical Society of America, 139(4)

ISSN

0001-4966

Authors

Thode, Aaron M
Kim, Katherine H
Norman, Robert G
[et al.](#)

Publication Date

2016-04-01

DOI

10.1121/1.4946011

Peer reviewed

Acoustic vector sensor beamforming reduces masking from underwater industrial noise during passive monitoring

Aaron M. Thode, Katherine H. Kim, Robert G. Norman, Susanna B. Blackwell, and Charles R. Greene Jr. WS

Citation: [The Journal of the Acoustical Society of America](#) **139**, EL105 (2016); doi: 10.1121/1.4946011

View online: <http://dx.doi.org/10.1121/1.4946011>

View Table of Contents: <http://asa.scitation.org/toc/jas/139/4>

Published by the [Acoustical Society of America](#)

Articles you may be interested in

[Normal mode solutions for seismo-acoustic propagation resulting from shear and combined wave point sources](#)

[The Journal of the Acoustical Society of America](#) **139**, (2016); 10.1121/1.4944752

[Rotational speed invariant fault diagnosis in bearings using vibration signal imaging and local binary patterns](#)

[The Journal of the Acoustical Society of America](#) **139**, (2016); 10.1121/1.4945818

[Flux projection beamforming for monochromatic source localization in enclosed space](#)

[The Journal of the Acoustical Society of America](#) **141**, (2017); 10.1121/1.4973193

[Determination of acoustic waveguide invariant using ships as sources of opportunity in a shallow water marine environment](#)

[The Journal of the Acoustical Society of America](#) **141**, (2017); 10.1121/1.4976112

[Sound source localization identification accuracy: Level and duration dependencies](#)

[The Journal of the Acoustical Society of America](#) **140**, (2016); 10.1121/1.4954870

[Compressive acoustic sound speed profile estimation](#)

[The Journal of the Acoustical Society of America](#) **139**, (2016); 10.1121/1.4943784

Acoustic vector sensor beamforming reduces masking from underwater industrial noise during passive monitoring

Aaron M. Thode^{a)}

Marine Physical Laboratory, Scripps Institution of Oceanography, San Diego,
California 92093-0205, USA
athode@ucsd.edu

Katherine H. Kim, Robert G. Norman, Susanna B. Blackwell, and
Charles R. Greene, Jr.

Greeneridge Sciences, Inc., 90 Dean Arnold Place, Suite D, Santa Barbara,
California 93117, USA
khkim@greeneridge.com, bobnorman@greeneridge.com, susanna@greeneridge.com,
cgreene@greeneridge.com

Abstract: Masking from industrial noise can hamper the ability to detect marine mammal sounds near industrial operations, whenever conventional (pressure sensor) hydrophones are used for passive acoustic monitoring. Using data collected from an autonomous recorder with directional capabilities (Directional Autonomous Seafloor Acoustic Recorder), deployed 4.1 km from an arctic drilling site in 2012, the authors demonstrate how conventional beamforming on an acoustic vector sensor can be used to suppress noise arriving from a narrow sector of geographic azimuths. Improvements in signal-to-noise ratio of up to 15 dB are demonstrated on bowhead whale calls, which were otherwise undetectable using conventional hydrophones.

© 2016 Acoustical Society of America

[WS]

Date Received: June 11, 2015 Date Accepted: March 31, 2016

1. Introduction

Passive acoustics has been increasingly used to detect underwater biological sounds to ascertain the presence of marine mammals during various industrial activities, using both real-time and autonomous equipment (McDonald *et al.*, 1995; Di Iorio and Clark, 2010; Thode *et al.*, 2012; Blackwell *et al.*, 2007). Conventional pressure-sensing hydrophones have been the primary sensor of choice for such monitoring studies. A major limitation of passive acoustic monitoring is that noise from the industrial operations themselves can interfere with, or “mask,” the detection of lower intensity biological sounds of interest. For example, vessel operations near an oil production island in the Beaufort Sea raised background levels by more than 20 dB over ambient levels (Blackwell and Greene, 2006). Similarly, reverberation from airgun pulses during seismic exploration increased background noise by 30–45 dB within 1 km of the seismic ship (Guerra *et al.*, 2011).

If the number of interfering noise sources is relatively small, then much of the masking noise will arrive from a small azimuthal swath relative to a receiver—the exact azimuthal spread depending on both the spatial extent of the activity and the distance of the recording hydrophone from the activity. Unfortunately, conventional hydrophones are usually designed to be omnidirectional across bandwidths of biological interest, which means that they are unable to reject noise originating from particular directions. A mature literature exists on using spatial arrays of hydrophones to reduce directional noise interference (Widrow *et al.*, 1967; Van Trees, 2004), but their effectiveness is highly frequency-dependent, and deploying the required two-dimensional (2D) spatial geometry on the ocean floor or in mid-water is logistically difficult.

Here we demonstrate how an acoustic vector sensor can suppress oil platform drilling noise to such an extent that bowhead whale calls, initially undetectable using the recorders’ omnidirectional hydrophone, become accessible once processed on a vector sensor. An acoustic vector sensor (D’Spain, 1990; Hawkes and Nehorai, 1998;

^{a)} Author to whom correspondence should be addressed.

McDonald, 2004; D'Spain *et al.*, 2006; Thode *et al.*, 2010) simultaneously measures acoustic pressure as well as particle velocity along one to three orthogonal axes. A signal with high signal-to-noise ratio (SNR) can have its azimuth directly inferred from the relative active acoustic intensities measured along each orthogonal axis (D'Spain *et al.*, 1991). For weaker signals, the time series can also be linearly combined to produce a directional beam pattern (McDonald, 2004; D'Spain *et al.*, 2006). If p , v_x , and v_y represent signal time series from a 2D vector sensor with omnidirectional (p) and two orthogonal particle velocity (v_x and v_y) sensors oriented such that the axis orthogonal to both v_x and v_y is vertical (pointing up), then a standard beamforming procedure is to compute

$$B(t, \theta) = p(t) - Z_0[v_x(t) \sin \theta + v_y(t) \cos \theta], \quad (1)$$

where θ is defined as an angle increasing clockwise relative to the internal x axis of the sensor, consistent with a geographic azimuth. (0° points to true or geodetic north, and θ increases clockwise, such that 90° is geodetic east.) In beamforming parlance, θ is often referred to as the “steering angle.” The free-space impedance Z_0 is a conversion factor that ensures that all three terms share the same units and scaling. Since the relationship between acoustic pressure and particle velocity in an acoustic plane wave is $v = p/\rho_0 c$, where ρ_0 and c are the respective density and sound speed of the fluid medium surrounding the sensor, a common value of Z_0 is typically $\rho_0 c$.

The exact form of Eq. (1) has been chosen so that if v_x and v_y are components of an acoustic plane wave arriving from angle θ_I , then B is zero whenever $\theta = \theta_I$. Figure 1(a) shows a logarithmic (dB) polar plot of the “cardioid” beam pattern resulting from Eq. (1), where v_x and v_y are aligned with the 0° and 90° axes, and an acoustic plane wave is arriving from a geodetic 45° azimuth in a noiseless environment. The beamformer output has been normalized so that the maximum output (which occurs at 225°) is 0 dB with respect to the incoming plane wave. Thus a plane wave arriving from 225° would suffer no attenuation after passing through the beamformer listed in Eq. (1), while a plane wave arriving from 45° is completely attenuated.

Previous applications of vector sensors in bioacoustics have emphasized how Eq. (1) and Fig. 1(a) can be used to determine the arrival direction of a signal of interest embedded in diffuse isotropic noise; namely, the angle that maximizes the output of Eq. (1) is the azimuth that the signal is propagating *toward* (or is 180° from the azimuth the signal is arriving *from*). Thus Eq. (1) can be used to determine the individual azimuths from which both industrial noise and unmasked biological signals are arriving.

However, Fig. 1(a) can also be interpreted as showing how this simple beamformer can suppress acoustic noise arriving from certain azimuths. This suppression is typically quantified by an array gain (AG), which is the ratio of the SNR of beamformer output over input (Urlick, 1983). An AG value greater than 0 dB indicates that noise has been suppressed relative to a signal of interest. The theoretical AG of a three-element vector sensor using Eq. (1) is 4.77 dB for a signal in isotropic noise

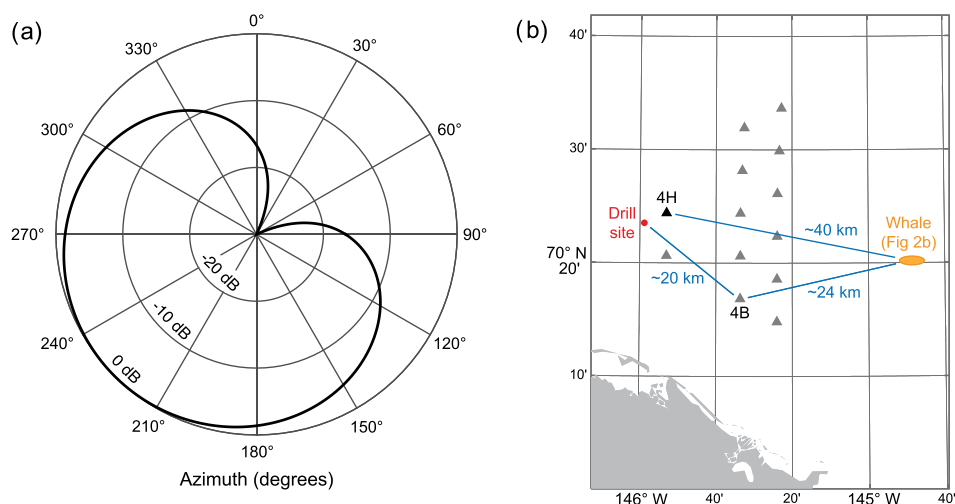


Fig. 1. (Color online) (a) Cardioid beam pattern generated by Eq. (1), for an interfering acoustic plane wave arriving from 45° and for $\theta = 45^\circ$ in a noiseless environment. The radial units show the dB reduction in noise amplitude, relative to the amplitude of the incoming noise. (b) Map of relative locations of drilling site, DASARs 4B and 4H, and whale signals shown in subsequent figures. DASAR 4H is 4 km from the drilling site.

(D'Spain *et al.*, 2006); however, for directional noise sources the effective AG can be much larger. For example, Fig. 1(a) illustrates that any noise arriving from roughly the same quadrant as the plane wave (0° – 90°) is reduced by at least 15 dB. Previous work on vector sensors (D'Spain *et al.*, 2006) has discussed how more sophisticated adaptive beamforming algorithms could be used to suppress sound arriving from two distinct directions. However, for the case of a single directional noise source, the broad response of the cardioid beamformer in Fig. 1(a) can be sufficient: it suppresses acoustic noise arriving from a relatively narrow azimuthal sector, but broadly preserves signals arriving from most other directions (e.g., signals are suppressed less than 10 dB over a 220° swath between roughly 118° and 332°). Thus, by an appropriate selection of θ in Eq. (1) (“steering the null”), directional industrial noise can be suppressed, potentially increasing the SNR of signals arriving from other directions by amounts greater than 4.77 dB. The appropriate value of θ can be discerned by finding the value of θ that maximizes Eq. (1), when applied to a sample of noise alone. The optimum azimuth for suppressing the noise will then be $\theta^\circ - 180^\circ$. The method is most effective whenever the angular noise distribution from the industrial activity (including bottom reverberation) is relatively narrow, and the signals of interest arrive from azimuths greater than 90° from those of the interfering noise.

2. Experimental results

2.1 Instrumentation

The suppression methods described above were tested on data collected by custom built Directional Autonomous Seafloor Acoustic Recorders, model C (DASAR-C) (Greene *et al.*, 2004; Thode *et al.*, 2012; Blackwell *et al.*, 2013). DASARs are equipped with an omnidirectional hydrophone and two orthogonal accelerometers that measure the north–south and east–west components of acoustic particle velocity at frequencies between 10 and 500 Hz. The hydrophone sensitivity (including all amplification to the A/D converter) is -149 dB re $1 \text{ V}/\mu\text{Pa}$ @ 100 Hz, while the sensitivity of the directional components is -97.5 dB re $1 \text{ (m/s)}/\text{V}$ @ 100 Hz. Incorporating the appropriate impedance value of Z_0 for a plane wave yields an equivalent pressure sensitivity of -146 dB re $1 \text{ V}/\mu\text{Pa}$ for these components. Over the band of interest (10 to 450 Hz) the sensitivity of all channels increases by 6 dB per octave. The noise floor spectral density of the hydrophone system is 10 dB below Knudsen sea state 0 conditions (42 dB re $1 \mu\text{Pa}^2/\text{Hz}$), while the equivalent noise floor for the velocity channels is about 6 dB higher. In the discussion that follows, all acoustic data (industrial noise and whale calls) were well above the instrument’s self-noise floor.

As explained in Greene *et al.* (2004), the geographic orientation of the sensors on the ocean floor was determined by transmitting frequency-modulated (FM) sweeps, tones, and pseudo-random noise at a set of known locations surrounding the sensor. The derived azimuths relative to the sensors could then be rotated by a correction angle (the azimuth between true north and the sensor y axis) to yield the geographic azimuth of the steering angle θ .

2.2 Location and industrial activity

The noise-canceling procedure was tested on data collected by several DASARs deployed in the Beaufort Sea in 2012, at water depths between 28 and 47 m. The DASARs were deployed in a triangular grid near the drill barge *Kulluk*, which was stationed near 70.39° N, 145.98° W. Data were examined from 13 DASARs, located between 4.1 and 29 km from the drilling site, but the figures shown here are restricted to the DASAR closest to the drilling location: DASAR 4H, at 4.1 km range (Blackwell *et al.*, 2015) and 63° relative to the drilling site. From the perspective of DASAR 4H the drilling site was at 243° azimuth [Fig. 1(b)]. Data were examined between 19:00 and 20:00 AKDT on October 3, 2012, a period that encompassed drilling activities which raised background noise levels by 10 to 15 dB at 4 km range from the *Kulluk*.

2.3 Example of noise suppression

Figure 2(a) shows received pressure levels of the conventional hydrophone at DASAR 4H for a 20-s period beginning at 19:07 AKDT, just before drilling activity at the site was officially logged. The noise interference consists of broadband diffuse noise between 70 and 85 dB re $1 \mu\text{Pa}^2/\text{Hz}$, resulting in substantial masking of signals between 20 and 400 Hz.

Figure 2(b) shows the same result after the three data channels from DASAR 4H were processed according to Eq. (1), with θ selected to correspond with a

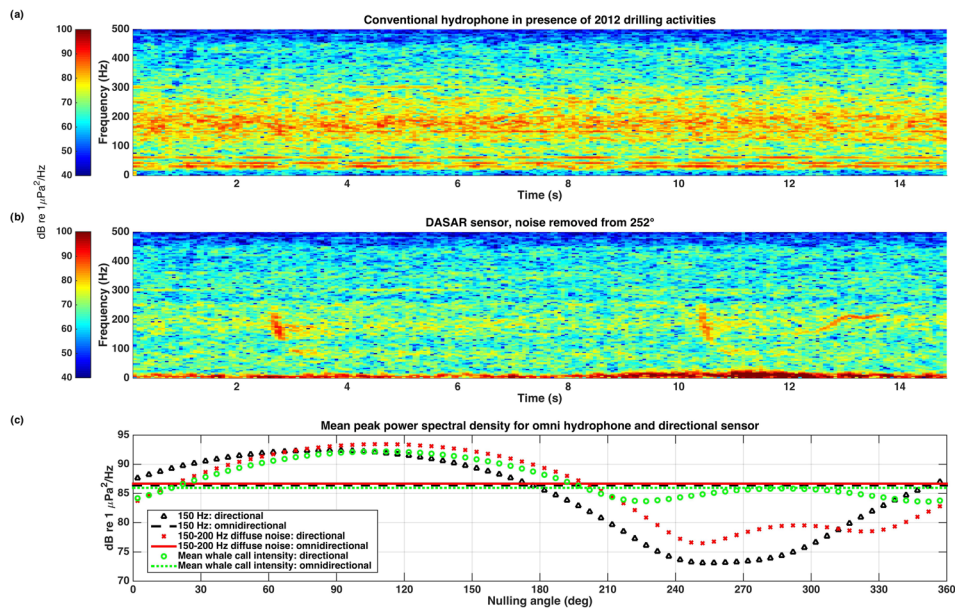


Fig. 2. (Color online) Example of DASAR noise cancellation of industrial activity beginning at 19:07 AKDT, October 3, 2012. (a) Spectrogram of conventional hydrophone output at DASAR 4H, a location 4.1 km from drilling site (256 pt fast Fourier transform, 75% overlap, 1 kHz sampling rate). (b) Spectrogram of output of Eq. (1), with θ selected to correspond to a geographic azimuth of 252° (maximum suppression of acoustic energy propagating from 252°). A bowhead whale call is detectable between 12 and 14 s. The other FM downsweeps are distant airgun signals from Canadian waters. Color bars are in terms of PSD, dB re $1 \mu\text{Pa}^2/\text{Hz}$. (c) Power spectral densities of both noise and whale signal, as a function of steering angle θ . Horizontal lines are outputs of a conventional hydrophone. Dashed line/triangles represent mean PSD of the 150 Hz tone (the peak frequency of industrial noise). Solid line/crosses represent mean peak PSD for noise sample (0 to 2 s) between 150 and 200 Hz. Dotted line/circles represent mean peak PSD of whale call between 150 and 200 Hz. The whale call SNR (in dB) is the difference between the circles and crosses. The azimuth of the drilling rig *Kulluk*, relative to the DASAR, is 243° .

geographic azimuth of 252° , roughly the azimuth of the drilling site with respect to 4H. A bowhead whale call between 12 and 14 s, previously undetected using the conventional hydrophone, is now visible between 150 and 200 Hz. Distant airgun signals from Canadian waters are also now visible at about 3 and 11 s.

Figure 2(c) shows how the mean beamformed intensities of the whale signal and two bandwidths of industrial noise vary with the value of θ . The corresponding intensities from the conventional hydrophone are plotted as horizontal lines. The mean intensity was computed from the power spectral density (PSD) spectrograms in Figs. 2(a) and 2(b) by locating the peak PSD for each spectrogram across frequency, and then taking the mean value of the resulting peak intensities over selected time windows. This approach was judged the best way to quantify improvements in the SNR of frequency-modulated bowhead calls.

The SNR of the whale call, which covers the same bandwidth as the broadband noise measurement, improves substantially after DASAR beamforming. The originally undetectable whale call in Fig. 2(b) has a maximum output SNR of 8.4 dB, after steering the null of the DASAR sensor to 252° , the drill site azimuth. Figure 2(c) shows how the noise levels (cross symbols) are minimized at a 252° steering angle. The whale call azimuth can be seen to be propagating toward 285° (arriving from $285^\circ - 180^\circ = 105^\circ$), since 285° maximizes the mean whale call intensity from the beamformer in that quadrant.

The same beamforming was performed on the 12 other DASARs in the area. Without beamforming, only 5 DASARs could detect the call, and those recorders were all greater than 20 km from the drill site. Using triangulation, these 5 recorders yielded a call location of 40 km range and 103° azimuth relative to DASAR 4H [Fig. 1(b)], consistent with the azimuths discussed in the previous paragraph.

Of these 5 recorders, DASAR 4B had the largest SNR of 8 dB. That instrument was located 20 km away from the drilling location, and 24 km away from the whale [Fig. 1(b)]. Sound source verification studies of seismic airgun surveys in nearby Camden Bay in 2007 (Funk et al., 2008) found an approximate transmission loss formula of 15 or $20 \cdot \log_{10}(R)$, where R is the source distance (in meters), and the transmission loss is in terms of dB. We thus estimate that the received level of the whale call on DASAR 4H was 3 dB lower than the same call detected on 4B

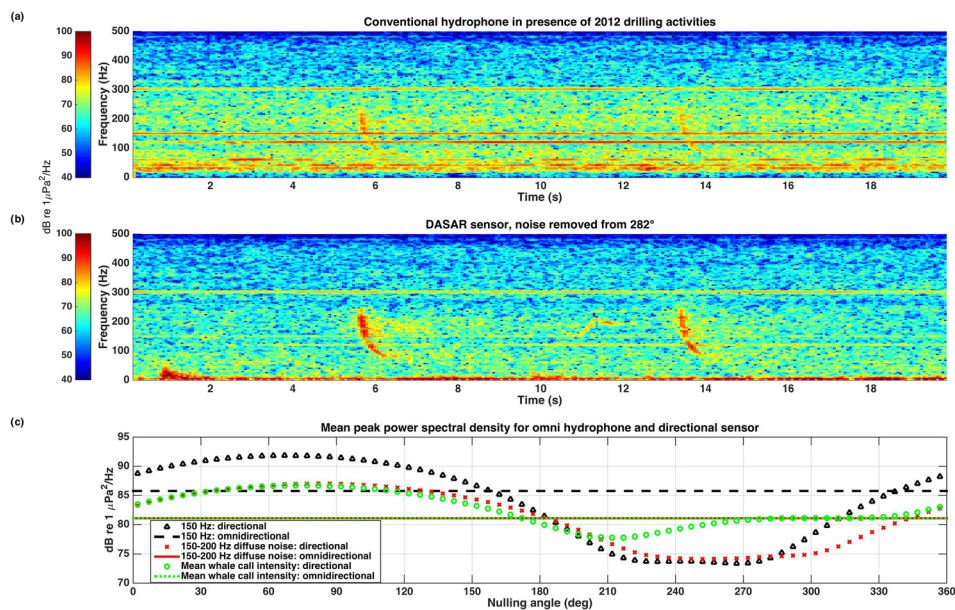


Fig. 3. (Color online) Example of DASAR noise cancellation of drilling activity beginning at 19:30 AKDT, October 3, 2012. (a) Spectrogram of conventional hydrophone output at DASAR 4H. (b) Spectrogram of output of Eq. (1), with θ selected to correspond to a geographic azimuth of 285°. A bowhead whale call is detectable between 11 and 12 s. The other FM downsweeps are distant airgun signals from Canadian waters. Color bars are in terms of PSD, dB re 1 $\mu\text{Pa}^2/\text{Hz}$. (c) Same style as Fig. 2(c), but displaying data analyzed from (a) and (b).

[i.e., $15 \times \log_{10}(24 \text{ km}/40 \text{ km}) \cong -3 \text{ dB}$]. We also find (from direct measurement) that the received noise levels at 4H are 11 dB greater than at 4B. We thus estimate that the initial SNR of the whale call on DASAR 4H was roughly $8 - 11 - 3 = -6 \text{ dB}$ prior to beamforming. Given that the measured SNR after beamforming was 8.4 dB, we conclude that beamforming the call increased its SNR by nearly 15 dB (from -6 to 8.4 dB). Using beamforming, this same call was detected on 11 of the 12 recorders (with the one failure arising from masking by the distant airgun signals).

Figure 3, analogous to Fig. 2, depicts another example of noise suppression, taken from 19:30 AKDT, when distinct tones from industrial activity are now visible at 150 and 300 Hz (90 dB re 1 $\mu\text{Pa}^2/\text{Hz}$). The whale call properties are measured between 11 and 13 s. For the case of the 150 Hz tone visible in Fig. 3(a), beamforming reduced its amplitude by 12 dB relative to the omnidirectional signal [74 dB vs 86 dB re 1 μPa ; triangles and long dashes in Fig. 3(c)], using data from the first 2 s of Fig. 3(a).

The angular distribution of the diffuse broadband noise between 150 and 200 Hz [crosses in Fig. 3(c)], measured between 7 and 9 s in Fig. 3(a), shows a similar angular distribution as the tone, although the broadband noise suppression is not as dramatic: 7 dB at 243°. The azimuth of maximum noise reduction for the broadband noise is coincident with the drill site's azimuth of 243° (relative to DASAR 4H), and the 150 Hz tone's azimuth is within 30° of this position. These angular differences may arise from support vessels that surrounded the *Kulluk*, but might also be attributable to bottom reverberation.

For an omnidirectional phone, the estimated SNR is 0 dB or less (the difference between the green dashed line and red solid line), while applying noise suppression at 282° yields a maximum SNR of 6.5 dB (difference between circles and crosses). As the contrasting spectrograms in Figs. 3(a) and 3(b) demonstrate, this SNR improvement yields a substantial difference in terms of visual acuity. Unlike Fig. 2(c), the azimuth of the whale call cannot be easily estimated from Fig. 3(c). Noise levels are sufficiently high that an uncontaminated local maximum in the circles in Fig. 3(c) does not exist, so the direction the whale call signal is propagating toward cannot be determined. However, triangulation of this call's location from other, more distant, DASARs yielded a 60 km distance from DASAR 4H at an azimuth of 99°.

3. Conclusion

Directional (vector) acoustic sensors can use conventional beamforming techniques to not only estimate the azimuthal arrival direction of biological signals, but also to suppress interfering noise arriving from a specific azimuth. The degree of

suppression depends on the angular distribution of the noise, which in turn is impacted by various factors, including the degree of bottom reverberation present in the interference. Nevertheless, measurements taken in the vicinity of oil drilling activity off the North Slope of Alaska show that the SNR of bowhead whale calls can be boosted by nearly 15 dB in relatively shallow water, depending on the azimuthal separation between the whale call and interfering noise. This increase in SNR enabled signals initially only detectable at ranges far from the drill site (greater than 20 km) to become detectable 4 km from the drill site (the closest DASAR data available). These noise suppression techniques could be incorporated in principle into a real-time system, as long as all three data channels of a DASAR instrument could be transmitted to a remote site. Equation (1) can be used to rapidly identify the azimuth of a directional noise source (by identifying the azimuth that maximizes the noise intensity), and then the noise can be suppressed by steering the beamformer 180° from that azimuth.

While the beamforming algorithm presented here helps unmask signals, it does not guarantee that the azimuths of those signals can be determined. Under certain circumstances [e.g., Fig. 2(c)], call azimuths could be estimated by noting at what angle the beamforming output from the call is maximized, and then subtracting 180° from this result. However, this approach only works when the signal's azimuth substantially differs from the azimuth of the interfering noise, and sometimes not even then [e.g., Fig. 3(c)]. More sophisticated algorithms using adaptive noise cancellation might permit both noise cancellation and azimuth estimation to be conducted more robustly.

Acknowledgments

This work was supported by Shell Exploration and Production Company (SEPCO). We thank the crew of the R/V *Norseman II* for tireless and professional support in the deployment and retrieval of the DASARs.

References and links

- Blackwell, S. B., and Greene, C. R., Jr. (2006). "Sounds from an oil production island in the Beaufort Sea in summer: Characteristics and contribution of vessels," *J. Acoust. Soc. Am.* **119**, 182–196.
- Blackwell, S. B., Nations, C. S., McDonald, T. L., Greene, C. R., Jr., Thode, A. M., Guerra, M., and Macrander, A. M. (2013). "Effects of airgun sounds on bowhead whale calling rates in the Alaskan Beaufort Sea," *Marine Mammal Sci.* **29**, E342–E365.
- Blackwell, S. B., Nations, C. S., McDonald, T. L., Thode, A. M., Mathias, D., Kim, K. H., Greene, C. R., Jr., and Macrander, A. M. (2015). "Effects of airgun sounds on bowhead whale calling rates: Evidence for two behavioral thresholds," *PLoS One* **10**(6), e0125720.
- Blackwell, S. B., Richardson, W. J., Greene, C. R., Jr., and Streever, B. (2007). "Bowhead whale (*Balaena mysticetus*) migration and calling behaviour in the Alaskan Beaufort Sea, Autumn 2001-04: An acoustic localization study," *Arctic* **60**, 255–270.
- Di Iorio, L., and Clark, C. W. (2010). "Exposure to seismic survey alters blue whale acoustic communication," *Biol. Letters* **6**, 51–54.
- D'Spain, G. L. (1990). "Energetics of the ocean's infrasonic sound field," Ph.D. thesis, University of California, San Diego, CA.
- D'Spain, G. L., Hodgkiss, W. S., and Edmonds, G. L. (1991). "Energetics of the deep ocean's infrasonic sound field," *J. Acoust. Soc. Am.* **89**, 1134–1158.
- D'Spain, G. L., Luby, J. C., Wilson, G. R., and Gramann, R. A. (2006). "Vector sensors and vector sensor line arrays: Comments on optimal array gain and detection," *J. Acoust. Soc. Am.* **120**, 171–185.
- Funk, D., Hannay, D., Ireland, D., Rodrigues, R., and Koski, W. (eds.) (2008). "Marine mammal monitoring and mitigation during open water seismic exploration by Shell Offshore Inc. in the Chukchi and Beaufort Seas, July–November 2007: 90-day report," LGL Rep. P969-1. Rep. from LGL Alaska Research Associates Inc., LGL Ltd., and JASCO Research Ltd. for Shell Offshore Inc., Nat. Mar. Fish. Serv., and U.S. Fish and Wild. Serv., 218 pp. plus Appendixes.
- Greene, C. R., Jr., McLennan, M. W., Norman, R. G., McDonald, T. L., Jakubczak, R. S., and Richardson, W. J. (2004). "Directional frequency and recording (DIFAR) sensors in seafloor recorders to locate calling bowhead whales during their fall migration," *J. Acoust. Soc. Am.* **116**, 799–813.
- Guerra, M., Thode, A. M., Blackwell, S. B., and Macrander, A. M. (2011). "Quantifying seismic survey reverberation off the Alaskan North Slope," *J. Acoust. Soc. Am.* **130**, 3046–3058.
- Hawkes, M., and Nehorai, A. (1998). "Acoustic vector-sensor beamforming and Capon direction estimation," *IEEE Trans. Signal Process.* **46**, 2291–2304.
- McDonald, M. A. (2004). "DIFAR hydrophone usage in whale research," *Can. Acoust.* **32**, 155–160.
- McDonald, M. A., Hildebrand, J. A., and Webb, S. C. (1995). "Blue and fin whales observed on a seafloor array in the Northeast Pacific," *J. Acoust. Soc. Am.* **98**, 712–721.
- Thode, A., Skinner, J., Scott, P., Roswell, J., Straley, J., and Folkert, K. (2010). "Tracking sperm whales with a towed acoustic vector sensor," *J. Acoust. Soc. Am.* **128**, 2681–2694.

- Thode, A. M., Kim, K. H., Blackwell, S. B., Greene, C. R., Jr., and Macrander, M. A. (2012). "Automated detection and localization of bowhead whale sounds in the presence of seismic airgun surveys," *J. Acoust. Soc. Am.* **131**, 3726–3747.
- Urick, R. J. (1983). *Principles of Underwater Sound* (Peninsula Publishing, Los Altos, CA).
- Van Trees, H. L. (2004). *Detection, Estimation, and Modulation Theory, Optimum Array Processing* (John Wiley & Sons, New York).
- Widrow, B., Mantey, P., Griffiths, L., and Goode, B. (1967). "Adaptive antenna systems," *J. Acoust. Soc. Am.* **42**, 1175–1176.